arXiv:1310.3348v1 [hep-ph] 12 Oct 2013

OCU-PHYS-390

125 GeV Higgs Boson and TeV Scale Colored Fermions in Gauge-Higgs Unification

Nobuhito Maru[a] and Nobuchika Okada[b]

[a] *Department of Mathematics and Physics, Osaka City University, Osaka 558-8585, Japan*

[b] *Department of Physics and Astronomy, University of Alabama, Tuscaloosa, Alabama 35487, USA*

Abstract

In the context of a simple gauge-Higgs unification scenario based on the gauge group $SU(3)\times U(1)'$ in a 5-dimensional flat spacetime, we investigate a possibility to realize the Higgs boson mass of 125 GeV with a compactification scale at the TeV. With the introduction of colored bulk fermions in a certain representation under the gauge group with a half-periodic boundary condition, we analyze the one-loop RGE of the Higgs quartic coupling with the gauge-Higgs condition and successfully obtain 125 GeV Higgs boson mass by adjusting a bulk mass for the fermions with a fixed compactification scale. The Kaluza-Klein modes of the colored fermions contribute to the Higgs-to-digluon effective coupling through the one-loop corrections. Since the contribution is destructive to the Standard Model one and reduces the Higgs boson production cross section, the recent LHC result gives a lower bound on the mass of the lightest Kaluza-Klein mode fermion. We find the mass of the lightest Kaluza-Klein mode fermion in the range of $2-3$ TeV for $10\%-5\%$ reductions of the Higgs boson production cross section through the gluon fusion channel. Such Kaluza-Klein mode fermions can be discovered at the LHC run II with $\sqrt{s}=13-14$ TeV, and LHC phenomenology for the Kaluza-Klein fermions is briefly discussed.

1 Introduction

The discovery of the long-sought Higgs boson by ATLAS [1] and CMS [2] collaborations at the Large Hadron Collider (LHC) is a milestone in the history of particle physics. With the discovery, we have begun testing the Higgs sector of the Standard Model (SM). Although the observed data for a variety of Higgs boson decay modes are found to be mostly consistent with the SM expectations, we need more data for definite conclusions. In fact, the Higgs diphoton decay mode showed the signal strength considerably larger than the SM prediction. Since the Higgs-to-diphoton coupling arises at the quantum level even in the SM, there is a good chance that the deviation originates from a certain new physics effect. This has motivated many recent studies for explanation of the deviation in various extensions of the SM with supersymmetry [3] or without supersymmetry [4]. The excess persists in the updated ATLAS analysis [5], while the updated CMS analysis [6] gives a much lower value for the signal strength of the diphoton events than the previous one [2]. More precise measurements of the Higgs boson properties might be a clue to finding physics beyond the SM, although the current LHC data have no indication for it.

In this paper we consider the gauge-Higgs unification (GHU) scenario [7] as a candidate for physics beyond the SM. This scenario offers a solution to the gauge hierarchy problem without invoking supersymmetry, where the SM Higgs doublet is identified as an extra spatial component of the gauge field in higher dimensional theory. The scenario predicts various finite physical observables such as Higgs potential [8, 9], the partial decay widths of the Higgs boson to digluon and diphoton [10, 11, 12], the anomalous magnetic moment $g-2$ [13], and the electric dipole moment [14], thanks to the higher dimensional gauge symmetry, irrespective of the non-renormalizable theory.

In our previous work [12, 15], we have investigated a simple GHU model based on the $SU(3) \times U(1)'$ gauge group by introducing color-singlet bulk fermions in 10 or 15-representation under the $SU(3)$ with a half-periodic boundary condition. We have analyzed one-loop contributions of Kaluza-Klein (KK) modes to the Higgs-to-digluon and Higgs-to-diphoton couplings and have confirmed that the KK mode contributions are destructive to the SM contributions from corresponding SM particles in the model [10].

This is a remarkable feature of the GHU, closely related to the absence of the quadratic divergence in Higgs self-energy corrections. We have shown that the bulk fermions can enhance the Higgs-to-diphoton coupling with appropriately chosen electric charges [12]. The bulk fermions also play a crucial role to achieve a Higgs boson mass of around 125 GeV. Without the bulk fermions, Higgs boson mass is predicted to be too small, less than 100 GeV.

In the same context, we have also studied the KK mode contributions to the Higgs to $Z\gamma$ decay [15]. We have found a very striking result that the KK mode contributions at the 1-loop level do not exist and hence the effective Higgs to $Z\gamma$ coupling remains unchanged, irrespectively of the effective Higgs-to-diphoton coupling. This is because Z boson only couples with two different mass eigenstates while the Higgs boson and photon couple with the same mass eigenstates. As a result, there is no one-loop diagram with KK modes contributing to the effective Higgs-to-$Z\gamma$ coupling. This specific result originates from the basic structure of the GHU scenario, where the SM gauge group is embedded in a larger gauge group in extra-dimensions and the SM Higgs doublet is identified with the higher dimensional component of the bulk gauge field.

In this paper, we investigate the case that the new bulk fermions with the half periodic boundary condition are color triplets, instead of color singlet ones introduced in [12]. As has been studied in [12], we can realize the 125 GeV Higgs boson mass also in this case by adjusting the bulk mass for a fixed compactification scale, depending on the representation of the bulk fermions. However, since the colored KK modes contribute to the effective Higgs-to-digluon coupling destructively to the SM particle (top quark) contribution, the Higgs boson production cross section through the gluon fusion is dramatically reduced as the KK modes become light. As a result, the current LHC data for the Higgs boson production give the lower bound on the lightest KK mode mass. For a variety of representations under the $SU(3) \times U(1)'$ gauge group for the bulk fermions, we identify the model-parameter region which can reproduce the 125 GeV Higgs boson mass and satisfy the LHC constraint.

The plan of this paper is as follows. In the next section, we introduce a simple GHU model [16, 17] based on the gauge group $SU(3) \times U(1)'$ in a 5-dimensional flat spacetime

with an orbifold S^1/Z_2 compactification to the 5th spacial dimension. We consider the introduction of a variety of colored bulk fermions in the representations of $\mathbf{6}, \mathbf{8}, \mathbf{10}$ and $\mathbf{15}$ under the bulk $SU(3)$ gauge group, for which a half-periodic boundary condition is imposed. In this context, we estimate Higgs boson mass in a four dimensional effective theory approach developed in Ref. [18], where Higgs boson mass is calculated by solving 1-loop renormalization group equation (RGE) of the Higgs quartic coupling with the so-called gauge-Higgs condition [18]. Once the representation of the bulk fermions are fixed, we identify the model-parameter region so as to reproduce the 125 GeV Higgs boson mass. In Sec. 3, we study effects of the colored bulk fermions to Higgs-to-digluon and Higgs-to-diphoton couplings. We discuss the lower bound on the mass of the lightest KK mode fermions to be consistent with the LHC data for the Higgs boson signals. Sec. 4 is devoted to conclusions and discussions.

2 Higgs boson mass in simple GHU model

Let us consider a simple GHU model based on the gauge group $SU(3) \times U(1)'$ in a 5-dimensional flat spacetime with an orbifolding of the 5th dimension on S^1/Z_2 with radius R_c of S^1. In our setup of bulk fermions whose zero-modes correspond to the SM fermions, we follow Ref. [17]: the up-type quarks except for the top quark, the down-type quarks and the leptons are embedded, respectively, into $\mathbf{3}$, $\overline{\mathbf{6}}$, and $\mathbf{10}$ representations of $SU(3)$. In order to realize the large top Yukawa coupling, the top quark is embedded into a rank 4 representation of $SU(3)$, namely $\overline{\mathbf{15}}$. The extra $U(1)'$ symmetry works to yield the correct weak mixing angle, and the SM $U(1)_Y$ gauge boson is given by a linear combination between the gauge bosons of the $U(1)'$ and the $U(1)$ subgroup in $SU(3)$ [16][1]. We assign appropriate $U(1)'$ charges for bulk fermions to give the correct hypercharge for the SM fermions.

The boundary conditions should be suitably assigned to reproduce the SM fields as the zero modes. While a periodic boundary condition corresponding to S^1 is taken for all of the bulk SM fields, the Z_2 parity is assigned for gauge fields and fermions in the

[1] It is known that the correct Weinberg angle can be also obtained by introducing brane localized gauge kinetic terms [16], but we do not take this approach in this paper.

representation $\mathcal{R}$ by using the parity matrix $P = \mathrm{diag}(-,-,+)$ as

$$A_\mu(-y) = P^\dagger A_\mu(y) P, \quad A_y(-y) = -P^\dagger A_\mu(y) P, \quad \psi(-y) = \mathcal{R}(P)\psi(y) \tag{1}$$

where the subscripts μ (y) denotes the four (the fifth) dimensional component. With this choice of parities, the $SU(3)$ gauge symmetry is explicitly broken to $SU(2) \times U(1)$. A hypercharge is a linear combination of $U(1)$ and $U(1)'$ in this setup. Here, the $U(1)_X$ symmetry is anomalous in general and broken at the cutoff scale and hence, the $U(1)_X$ gauge boson has a mass of order of the cutoff scale [16]. As a result, zero-mode vector bosons in the model are only the SM gauge fields.

Off-diagonal blocks in A_y have zero modes because of the overall sign in Eq. (1), which corresponds to an $SU(2)$ doublet. In fact, the SM Higgs doublet (H) is identified as

$$A_y^{(0)} = \frac{1}{\sqrt{2}} \begin{pmatrix} 0 & H \\ H^\dagger & 0 \end{pmatrix}. \tag{2}$$

The KK modes of A_y are eaten by KK modes of the SM gauge bosons and enjoy their longitudinal degrees of freedom like the usual Higgs mechanism.

The parity assignment also provides the SM fermions as massless modes, but it also leaves exotic fermions massless. Such exotic fermions are made massive by introducing brane localized fermions with conjugate $SU(2) \times U(1)$ charges and an opposite chirality to the exotic fermions, allowing us to write mass terms on the orbifold fixed points. In the GHU scenario, the Yukawa interaction is unified with the gauge interaction, so that the SM fermions obtain the mass of the order of the W-boson mass after the electroweak symmetry breaking. To realize light SM fermion masses, one may introduce a Z_2-parity odd bulk mass terms for the SM fermions, except for the top quark. Then, zero mode fermion wave functions with opposite chirality are localized towards the opposite orbifold fixed points and as a result, their Yukawa coupling is exponentially suppressed by the overlap integral of the wave functions. In this way, all exotic fermion zero modes become heavy and small Yukawa couplings for light SM fermions are realized by adjusting the bulk mass parameters. In order to realize the top quark Yukawa coupling, we introduce a rank 4 symmetric tensor $\overline{\mathbf{15}}$ without a bulk mass [17]. This provide us with a group theoretical factor 2 for the coupling of the top quark with the Higgs doublet, so that we

have $m_t = 2m_W$ at the compactification scale [16]. Taking QCD threshold corrections to the top quark pole mass, this mass relation is desirable. See, for example, Ref. [19] for flavor mixing and CP violation in the GHU scenario.

Since it is a highly non-trivial task to propose a realistic GHU scenario (see, for example, Refs. [16, 17] toward this direction), we employ a four dimensional effective theory approach developed by Ref. [18] in estimating a Higgs boson mass. As has been shown in Ref. [18], the low energy effective theory of the 5-dimensional GHU scenario is equivalent to the SM with the so-called "gauge-Higgs condition" on the Higgs quartic coupling, namely, we impose a vanishing Higgs quartic coupling at the compactification scale. This boundary condition reflects the 5-dimensional gauge invariance and, once it is restored, the Higgs potential disappears. According to this effective theory approach, the Higgs boson mass at low energies is easily calculated from the RGE evolution of the Higgs quartic coupling below the compactification scale, under the the gauge-Higgs condition. Another advantage of this approach is that we can see that the GHU scenario offers a natural solution to the instability problem of the Higgs potential in the SM, because the potential vanishes at the compactification scale and remains zero at higher scales. We assume that the electroweak symmetry breaking correctly occurs by the introduction of a suitable set of bulk fermions. Note that the effective Higgs mass squared is quadratically sensitive to the mass of heavy states, while the effective Higgs quartic coupling is dominantly determined by interactions of the Higgs doublet with light states. Therefore, the Higgs boson mass at low energies is mainly determined by light states below the compactification scale, assuming the correct electroweak symmetry breaking.

In the following, we consider three different representations for the colored bulk fermions: $(\mathbf{3}, \mathbf{6})$, $(\mathbf{3}, \mathbf{10})$ and $(\mathbf{3}, \mathbf{15})$ under $SU(3)_c \times SU(3)$, with suitable $U(1)'$ charge assignments. The half periodic boundary condition is imposed on the bulk fermions, $\psi(y + 2\pi R) = -\psi(y)$. Thanks to the boundary condition, the model leads to no unwanted exotic massless fermion, while the lightest KK modes of the fermions are involved in the RGE evolutions since their masses are smaller than the compactification scale. We will see that the existence of the half-periodic bulk fermion is crucial to achieve a Higgs boson mass of around 125 GeV

Let us begin with the **6**-plet of $SU(3)$, which is decomposed into the representations under $SU(2) \times U(1)$ as

$$\mathbf{6} = \mathbf{1}_{-2/3} \oplus \mathbf{2}_{-1/6} \oplus \mathbf{3}_{1/3}, \tag{3}$$

where the numbers in the subscript denote the $U(1)$ charges. After the electroweak symmetry breaking the KK mass spectrum is found as follows:

$$\begin{aligned}
\left(m^{(\pm)}_{n,-2/3}\right)^2 &= \left(m_{n+\frac{1}{2}} \pm 2m_W\right)^2 + M^2, \quad m^2_{n+\frac{1}{2}} + M^2, \\
\left(m^{(\pm)}_{n,+1/3}\right)^2 &= \left(m_{n+\frac{1}{2}} \pm m_W\right)^2 + M^2, \\
\left(m^{(\pm)}_{n,+4/3}\right)^2 &= m^2_{n+\frac{1}{2}} + M^2,
\end{aligned} \tag{4}$$

where the numbers in the subscript denote the "electric charges"[2] of the corresponding KK mode fermions, $m_{n+\frac{1}{2}} = \left(n + \frac{1}{2}\right) M_{\rm KK}$ with $n = 0, 1, 2, \cdots$, $M_{\rm KK} \equiv 1/R_c$ and M is a bulk mass. In the same way, we decompose the **10**-plet as

$$\mathbf{10} = \mathbf{1}_{-1} \oplus \mathbf{2}_{-1/2} \oplus \mathbf{3}_0 \oplus \mathbf{4}_{1/2}. \tag{5}$$

The KK mass spectrum after the electroweak symmetry breaking is found as:

$$\begin{aligned}
\left(m^{(\pm)}_{n,-1}\right)^2 &= \left(m_{n+\frac{1}{2}} \pm 3m_W\right)^2 + M^2, \quad \left(m_{n+\frac{1}{2}} \pm m_W\right)^2 + M^2, \\
\left(m^{(\pm)}_{n,0}\right)^2 &= \left(m_{n+\frac{1}{2}} \pm 2m_W\right)^2 + M^2, \quad m^2_{n+\frac{1}{2}} + M^2, \\
\left(m^{(\pm)}_{n,+1}\right)^2 &= \left(m_{n+\frac{1}{2}} \pm m_W\right)^2 + M^2, \\
\left(m^{(\pm)}_{n,+2}\right)^2 &= m^2_{n+\frac{1}{2}} + M^2.
\end{aligned} \tag{6}$$

For the **15**-plet, the decomposition under $SU(2) \times U(1)$ is given by

$$\mathbf{15} = \mathbf{1}_{-4/3} \oplus \mathbf{2}_{-5/6} \oplus \mathbf{3}_{-1/3} \oplus \mathbf{4}_{1/6} \oplus \mathbf{5}_{2/3}. \tag{7}$$

[2] Here "electric charges" mean by electric charges of $SU(2) \times U(1) \subset SU(3)$. A true electric charge of each KK mode is given by a sum of the "electric charge" and $U(1)'$ charge Q.

After the electroweak symmetry breaking, the KK mass spectrum is found as follows:

$$\begin{aligned}
\left(m^{(\pm)}_{n,-4/3}\right)^2 &= \left(m_{n+\frac{1}{2}} \pm 4m_W\right)^2 + M^2, \quad \left(m_{n+\frac{1}{2}} \pm 2m_W\right)^2 + M^2, \quad m^2_{n+\frac{1}{2}} + M^2, \\
\left(m^{(\pm)}_{n,-1/3}\right)^2 &= \left(m_{n+\frac{1}{2}} \pm 3m_W\right)^2 + M^2, \quad \left(m_{n+\frac{1}{2}} \pm m_W\right)^2 + M^2, \\
\left(m^{(\pm)}_{n,2/3}\right)^2 &= \left(m_{n+\frac{1}{2}} \pm 2m_W\right)^2 + M^2, \quad m^2_{n+\frac{1}{2}} + M^2, \\
\left(m^{(\pm)}_{n,5/3}\right)^2 &= \left(m_{n+\frac{1}{2}} \pm m_W\right)^2 + M^2, \\
\left(m^{(\pm)}_{n,8/3}\right)^2 &= m^2_{n+\frac{1}{2}} + M^2.
\end{aligned} \tag{8}$$

In our model, we have introduced bulk fermions with the half-periodic boundary condition, and their first KK modes appear below the compactification scale. Therefore, not only the SM particles but also the first KK modes are involved in our RGE analysis with the gauge-Higgs condition.[3] The 1-loop RGE for the Higgs quartic coupling λ below the compactification scale is given by

$$\begin{aligned}
\frac{d\lambda}{d\ln\mu} &= \frac{1}{16\pi^2}\left[12\lambda^2 - \left(\frac{9}{5}g_1^2 + 9g_2^2\right)\lambda + \frac{9}{4}\left(\frac{3}{25}g_1^4 + \frac{2}{5}g_1^2g_2^2 + g_2^4\right)\right. \\
&\quad \left. +4\left(3y_t^2 + 3C_2(\mathbf{R})\left(\frac{g_2}{\sqrt{2}}\right)^2\right)\lambda - 4\left(3y_t^4 + 3C_4(\mathbf{R})\left(\frac{g_2}{\sqrt{2}}\right)^4\right)\right],
\end{aligned} \tag{9}$$

where y_t is the top Yukawa coupling, $g_{1,2}$ are the $SU(2)$, $U(1)_Y$ gauge couplings, respectively, and $C_2(\mathbf{R})$ and $C_4(\mathbf{R})$ are contributions to the beta function by the representation $\mathbf{R} = \mathbf{6}$, $\mathbf{10}$, and $\mathbf{15}$. In our RGE analysis, we neglect the KK mode mass splitting by the electroweak symmetry breaking and set the first KK mode mass as

$$m_0^{(\pm)} = \frac{1}{2}M_{\rm KK}\sqrt{1 + 4c_B^2} \tag{10}$$

where $c_B \equiv M/M_{\rm KK}$.

For the energy scale $m_0^{(\pm)} \leq \mu \leq M_{\rm KK}$, the coefficients $C_2(\mathbf{R})$ and $C_4(\mathbf{R})$ are explicitly

[3] In Ref. [20], the gauge-Higgs condition with only the SM particle contents below the compactification scale is used to predict Higgs boson mass as a function of the compactification scale.

given by

$$\begin{aligned} C_2(\mathbf{6}) &= 2\left(2^2+1^2\right), \\ C_4(\mathbf{6}) &= 2\left(2^4+1^4\right), \\ C_2(\mathbf{10}) &= 2\left(3^2+1^2+2^2+1^2\right), \\ C_4(\mathbf{10}) &= 2\left(3^4+1^4+2^4+1^4\right), \\ C_2(\mathbf{15}) &= 2\left(4^2+2^2+3^2+1^2+2^2+1^2\right), \\ C_4(\mathbf{15}) &= 2\left(4^4+2^4+3^4+1^4+2^4+1^4\right), \end{aligned} \tag{11}$$

while these coefficients are set to be 0 for $\mu < m_0^{(\pm)}$ since the first KK modes are decoupled at the scale $m_0^{(\pm)}$. In our analysis, the running effects for $y_t, g_{1,2}$ are simply neglected.

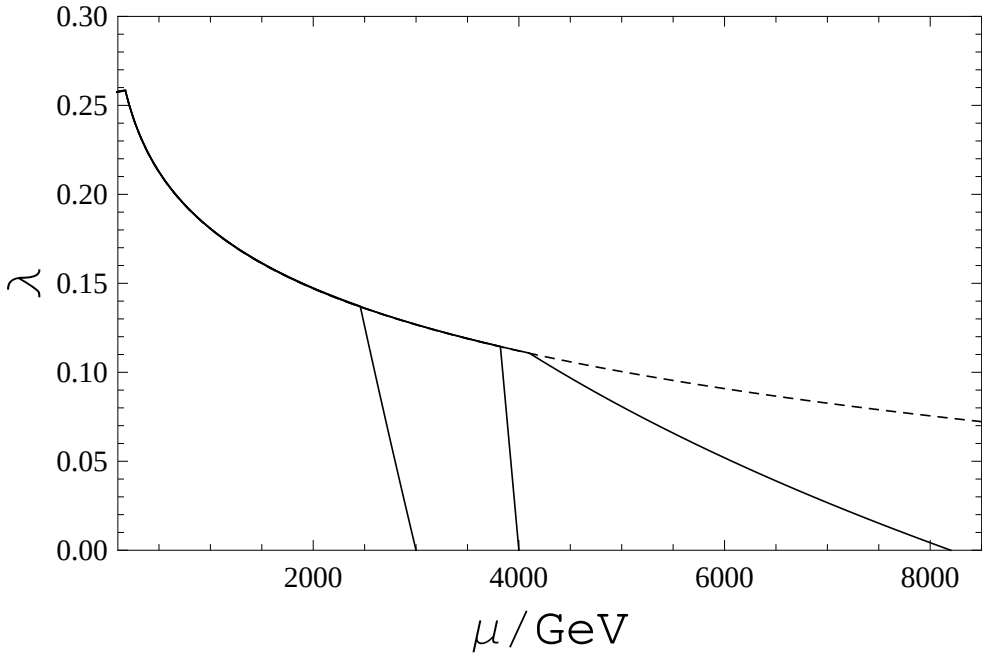


Figure 1: The RGE running of the Higgs quartic coupling at the 1-loop level. The three solid lines correspond, respectively, to the cases of the **6**-plet with $(M_{\rm KK}, m_0^{(\pm)}) = (8.2, 4.1)$ TeV, the **10**-plet with $(M_{\rm KK}, m_0^{(\pm)}) = (3.0, 2.46)$ TeV, the **15**-plet with $(M_{\rm KK}, m_0^{(\pm)}) = (4.0, 3.82)$ TeV. The dashed line shows the RGE running of the SM Higgs quartic coupling with the boundary condition, $\lambda(\mu = m_h) = 0.258$, corresponding to the Higgs pole mass $m_h = 125$ GeV.

The numerical solution to the 1-loop RGE of the Higgs quartic coupling are shown in Fig. 1. Here we have applied the gauge-Higgs condition at the compactification scales, $M_{\rm KK} = 8.2$, 3.5, and 4.0 TeV, respectively for **6**, **10**, and **15**-plets and numerically solve the RGE of Eq. (9) toward low energies. Here, we have used $y_t(\mu) = 0.944$ for $\mu \geq m_t = 173.2$ GeV ($y_t(\mu) = 0$ for $\mu < m_t = 173.2$ GeV), and $g_1 = 0.459$, and $g_2 = 0.649$ at the Z-boson mass scale. For simplicity, we estimate the Higgs boson pole mass by the condition $\lambda(\mu = m_h)v^2 = m_h^2$, which means $\lambda(\mu = m_h) = 0.258$ for $m_h = 125$ GeV. For a fixed compactification scale, we have adjusted the bulk mass M so as to reproduce the 125 GeV Higgs boson mass. Corresponding masses for the fist KK modes are found to be $m_0^{(\pm)} = 4.1, 2.46$ and 3.82 TeV, respectively, for **6**, **10**, and **15**-plets. In this rough analysis, the Higgs quartic coupling under the SM RGE evolution becomes zero at $\mu \simeq 3 \times 10^4$ GeV. As is well-known, in more precise analysis with higher order corrections (see, for example, [21]), the Higgs quartic coupling becomes zero at $\mu \simeq 10^{10}$ GeV. In the precise analysis, the running top Yukawa coupling is monotonically decreasing and the higher order corrections positively contribute to the beta function, as a result, the scale realizing $\lambda(\mu) = 0$ is pushed up to high energies.

As can be seen from Fig. 1, the existence of the half-periodic bulk fermions is essential to realize the 125 GeV Higgs boson mass with the compactification scale at the TeV. For a fixed compactification scale, we adjust the bulk mass to be the value at which the RGE solution with the bulk fermions merges with the SM RGE evolution toward high energies with the boundary condition $\lambda(\mu = m_h) = 0.258$. Since a higher dimensional bulk fermions provide more KK mode fermions in the SM decomposition, the running of Higgs quartic coupling is more sharply rising from zero toward low energies in the case with fermions in higher representations. In the viewpoint of the LHC physics, the **10** and **15**-plets are interesting since their first KK mode masses can be around a few TeV, while for the **6**-plet the KK mode mass is relatively higher. This is because the **6**-plet provides less number of the lightest KK mode fermions and a relatively larger compactification scale is required to reproduce the 125 GeV Higgs boson mass. In fact, we have found the lower bound, $M_{\rm KK} \geq 8.2$ TeV, for the case with the **6**-plet. We have also performed the same analysis for a bulk fermion of the **8**-plet and found the result very similar to the

6-plet case. Hereafter we will focus on two cases of **10** and **15**-plets.

Once the compactification scale is fixed, the bulk mass parameter (c_B) or equivalently, the lightest KK mode mass ($m_0^{(\pm)}$) is determined so as to reproduce the 125 GeV Higgs boson mass. The relation between $m_0^{(\pm)}$ and $M_{\rm KK}$ is shown in Fig. 2. The solid (dashed) line represents the resultant bulk mass $m_0^{(\pm)}$ of the **10**(**15**)-plet as a function of the compactification scale, $M_{\rm KK}$. We have found that the lightest KK mode mass $m_0^{(\pm)}$ are close to the compactification scale $M_{\rm KK}$.

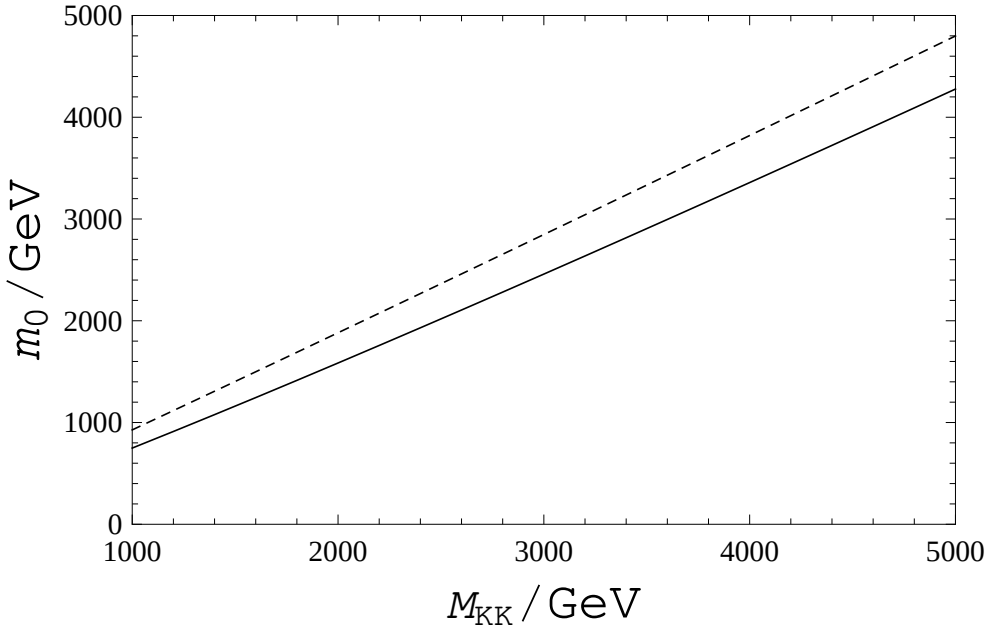


Figure 2: For the case of the **10**-plet (**15**-plet), the solid (dashed) line shows the relation between the lightest KK mode mass $m_0^{(\pm)}$ and the compactification scale $M_{\rm KK}$, along which $m_h = 125$ GeV is reproduced.

3 Higgs production and diphoton decay in GHU

The bulk colored fermions we have introduced contribute to the effective Higgs-to-digluon and diphoton couplings through 1-loop corrections [10, 12], so that the Higgs boson production cross section and its branching ratio can be altered from the SM values. In this

section, we evaluate the contributions from the bulk **10**-plet and **15**-plet fermions and discuss constraints for the model-parameters by the LHC data.

3.1 Higgs boson production through gluon fusion at the LHC

At the LHC, the Higgs boson is dominantly produced via gluon fusion process with the following dimension five operator between the Higgs boson and digluon:

$$\mathcal{L}_{\rm eff} = C_{gg} h G^a_{\mu\nu} G^{a\mu\nu} \tag{12}$$

where h is the SM Higgs boson, and $G^a_{\mu\nu}$ (a = 1-8) is the gluon field strength. The SM contribution to C_{gg} is dominated by top quark 1-loop corrections. As a good approximation, we express the contribution by using the Higgs low energy theorem [22],

$$C_{gg}^{\rm SMtop} \simeq \frac{g_3^2}{32\pi^2 v} b_3^t \frac{\partial}{\partial \log v} \log m_t = \frac{\alpha_s}{12\pi v} \tag{13}$$

where g_3 ($\alpha_s = g_3^2/(4\pi)$) is the QCD coupling constant (fine structure constant), m_t is a top quark mass, and $b_3^t = 2/3$ is a top quark contribution to the beta function coefficient of QCD.

In addition to the SM contribution, we take into account the contributions from the top quark KK-modes and the KK modes of the bulk **10**-plet or **15**-plet. As mentioned before, the SM top quark is embedded into the $\overline{\mathbf{15}}$-plet with a periodic boundary condition and its KK mass spectrum is given by [17]

$$m_{n,t}^{(\pm)} = m_n \pm m_t \tag{14}$$

where $m_t = 2m_W$ with the W-boson mass ($m_W = 80.4$ GeV), and $m_n \equiv n M_{\rm KK}$ with an integer $n = 1, 2, 3, \cdots$. Although the $\overline{\mathbf{15}}$-plet generally includes exotic massless fermions, we have assumed that all the exotic fermions are decoupled by adjusting large brane-localized mass terms with the brane fermions. Thus, we only consider KK modes of the SM top quark.[4] It is straightforward to calculate KK top contributions by using the Higgs

[4] One might think that the KK mode contributions from the light fermions should be taken into account. However, they can be safely neglected compared to those from the heavy fermions, since the total KK mode sum is proportional to the corresponding SM fermion masses generated by the electroweak symmetry breaking as is seen in (15) for instance.

low energy theorem:

$$C_{gg}^{\rm KKtop} \simeq \frac{\alpha_s}{12\pi v}\sum_{n=1}^{\infty}\frac{\partial}{\partial\log v}\left[\log(m_n+m_t)+\log(m_n-m_t)\right]$$
$$\simeq -\frac{\alpha_s}{12\pi v}2\sum_{n=1}^{\infty}\left(\frac{2m_W}{m_n}\right)^2 = -\frac{\alpha_s}{12\pi v}\times\frac{\pi^2}{3}\left(\frac{2m_W}{M_{\rm KK}}\right)^2, \quad (15)$$

where we have used $m_t = 2m_W$, an approximation of $m_W^2 \ll m_n^2$, and $\sum_{n=1}^{\infty} 1/n^2 = \pi^2/6$.

The **10**-plet or **15**-plet fermion with the half-periodic boundary condition has the KK mass spectrum as shown in Eqs. (6) and (8). Applying the Higgs low energy theorem, their contributions to the Higgs-to-digluon coupling are calculated as

$$C_{gg}^{\rm KK10} \simeq F(3m_W)+F(2m_W)+2F(m_W), \quad (16)$$
$$C_{gg}^{\rm KK15} \simeq F(4m_W)+F(3m_W)+2F(2m_W)+2F(m_W) \quad (17)$$

where the function $F(m_W)$ is given by [12]

$$F(m_W) = \frac{\alpha_s}{12\pi v}\sum_{n=1}^{\infty}\frac{\partial}{\partial\log v}\left[\log\sqrt{M^2+(m_{n+\frac{1}{2}}+m_W)^2}+\log\sqrt{M^2+(m_{n+\frac{1}{2}}-m_W)^2}\right]$$
$$\simeq -\frac{\alpha_s}{6\pi v}\left(\frac{m_W}{M_{\rm KK}}\right)^2\sum_{n=0}^{\infty}\frac{\left(n+\frac{1}{2}\right)^2-c_B^2}{\left(\left(n+\frac{1}{2}\right)^2+c_B^2\right)^2} = -\frac{\alpha_s}{12\pi v}\left(\frac{m_W}{M_{\rm KK}}\right)^2\frac{\pi^2}{\cosh(\pi c_B)}. \quad (18)$$

Here we have used the approximation $m_W^2 \ll M_{\rm KK}^2$.

As pointed out in [10], the KK mode contribution to the Higgs-to-digluon coupling is destructive to the SM one. This result originates from the mass splitting between $m_{n,t}^{(+)}$ and $m_{n,t}^{(-)}$ in Eq. (14) or between $m_{n,q}^{(+)}$ and $m_{n,q}^{(-)}$ in Eqs. (6) and (8), which are generated by the electroweak symmetry breaking.[5] This destructive contribution is a typical feature of the GHU, in sharp contrast with the one in the universal extra dimension models [23].

Now we evaluate the ratio of the Higgs production cross section through the gluon

[5] This mass splitting also plays a crucial role to make the KK-mode loop corrections finite. It has been shown [11] that this finiteness is valid for GHU in various space-time dimensions and at any perturbative level.

fusion at the LHC in our model to the SM one as

$$
\begin{aligned}
R_{gg} &\equiv \left(1+\frac{C_{gg}^{\rm KKtop}+C_{gg}^{\rm KK10(15)}}{C_{gg}^{\rm SMtop}}\right)^2 \\
&\simeq \begin{cases} \left(1-\frac{\pi^2}{3}\left(\frac{2m_W}{M_{\rm KK}}\right)^2-\left(\frac{m_W}{M_{\rm KK}}\right)^2\frac{15\pi^2}{\cosh(\pi c_B)}\right)^2 & \text{for } \mathbf{10}-\text{plet.} \\ \left(1-\frac{\pi^2}{3}\left(\frac{2m_W}{M_{\rm KK}}\right)^2-\left(\frac{m_W}{M_{\rm KK}}\right)^2\frac{25\pi^2}{\cosh(\pi c_B)}\right)^2 & \text{for } \mathbf{15}-\text{plet.} \end{cases}
\end{aligned}
\tag{19}
$$

As we have investigated in the previous section, in order to reproduce $m_h = 125$ GeV there is a relation between $M_{\rm KK}$ and $m_0^{(\pm)}$ (or equivalently, c_B) shown in Fig. 2. Thus, the ratio R_{gg} is described as a function of only the compactification scale $M_{\rm KK}$. The results are shown in Fig. 3.

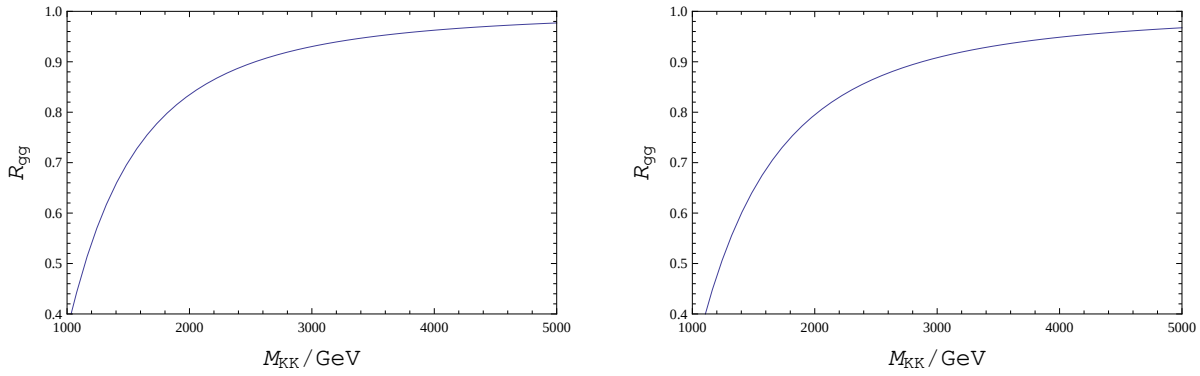


Figure 3: The ratio of the Higgs production cross section in our model to the SM one as a function of the compactification scale $M_{\rm KK}$. The left (right) panel corresponds to the **10**(**15**)-plet case. The bulk mass c_B is fixed as a function of $M_{\rm KK}$ (along the lines in Fig. 2) so as to reproduce $m_h = 125$ GeV.

Since the KK mode contribution to the Higgs production cross section is destructive to the SM process, the resultant cross section becomes smaller than the SM value as the compactification scale is lowered. The Higgs boson properties observed at the LHC experiments are mostly consistent with the SM expectations, so that the LHC data can provide a lower bound on the compactification scale not to make the Higgs boson production rate too small. The Higgs boson has couplings with the weak gauge bosons and SM fermions at the tree level, which the KK mode contribution to are negligible. Thus,

the signal strength for the process $gg \to h \to ZZ^*$, for example, is altered essentially by a change of the Higgs production cross section through the gluon fusion process. Although the current LHC result for the Higgs boson signal still allow a large deviation from the SM prediction, we here consider a constraint on the Higgs production cross section to be larger than 90 (95) % of the SM model prediction, $R_{gg} \geq 0.9$ ($R_{gg} \geq 0.95$). From Figs. 3 and 2, we can read off the lower bound on $M_{\rm KK}$ and $m_0^{(\pm)}$ for the case of the **10** and **15**-plets, respectively. With the lower bound on $M_{\rm KK}$ and $m_0^{(\pm)}$, we can calculate the lightest KK mode mass from the mass spectrum formulas in Eqs. (6) and (8). For the case of the **10**-plet, we have found the lightest KK mode mass as 1.9 TeV (2.4 TeV) for $R_{gg} = 0.9$ ($R_{gg} = 0.95$), while 2.5 TeV (2.7 TeV) for $R_{gg} = 0.9$ ($R_{gg} = 0.95$), for the case of the **15**-plet. The results are shown in Table 1. The lower bounds are found to be at TeV, so that such exotic colored particles can be discovered at the LHC Run II with $\sqrt{s} = 13 - 14$ TeV.

10-plet	$R_{gg} = 0.9$	$R_{gg} = 0.95$
$M_{\rm KK}$ (TeV)	2.54	3.45
$m_0^{(\pm)}$ (TeV)	2.05	2.91
$m_{\rm lightest}$ (TeV)	1.91	2.77
15-plet	$R_{gg} = 0.9$	$R_{gg} = 0.95$
$M_{\rm KK}$ (TeV)	2.88	4.05
$m_0^{(\pm)}$ (TeV)	2.73	3.87
$m_{\rm lightest}$ (TeV)	2.57	3.71

Table 1: The lower bound on the KK mode masses from $0.9 \leq R_{gg}$ and $0.95 \leq R_{gg}$ for the cases with the **10** and **15**-plets.

3.2 Higgs decay to diphoton

Next we calculate the KK model contributions to the Higgs-to-diphoton coupling of the dimension five operator,

$$\mathcal{L}_{\rm eff} = C_{\gamma\gamma} h F_{\mu\nu} F^{\mu\nu}, \tag{20}$$

where $F_{\mu\nu}$ denotes the photon field strength. The Higgs low energy theorem also allows us to extract the coefficient from the 1-loop RGE of the QED coupling. In the SM, the

diphoton coupling is induced by the top quark and W-boson loop corrections. In addition to it, we have the contributions from the KK modes of top quark, W-boson, and the **10**-plet or the **15**-plet.

We begin with the SM top loop contribution. As a good approximation, we have

$$C_{\gamma\gamma}^{\rm SMtop} \simeq \frac{e^2 b_1^t}{24\pi^2 v}\frac{\partial}{\partial \log v}\log m_t = \frac{2\alpha_{em}}{9\pi v}, \tag{21}$$

where $b_1 = (2/3)^2 \times 3 = 4/3$ is a top quark contribution to the QED beta function coefficient, and α_{em} is the fine structure constant. Corresponding KK top quark contribution is given by

$$\begin{aligned} C_{\gamma\gamma}^{\rm KKtop} &\simeq \frac{e^2 b_1^t}{24\pi^2 v}\sum_{n=1}^{\infty}\frac{\partial}{\partial \log v}\left[\log(m_n+m_t)+\log(m_n-m_t)\right] \\ &\simeq -\frac{2\alpha_{em}}{9\pi v}\times\frac{\pi^2}{3}\left(\frac{2m_W}{M_{\rm KK}}\right)^2. \end{aligned} \tag{22}$$

Similar to the Higgs-to-digluon coupling, the KK top contribution is destructive to the SM top contribution.

The SM W-boson loop contribution is calculated as

$$C_{\gamma\gamma}^{W} \simeq \frac{e^2}{32\pi^2 v} b_1^W \frac{\partial}{\partial \log v}\log m_W = -\frac{7\alpha_{em}}{8\pi v} \tag{23}$$

where $m_W = g_2 v/2$, and $b_1^W = -7$ is a W-boson contribution to the QED beta function coefficient. This is a rough estimation of the W-boson loop contributions since $4m_W^2/m_h^2 \gg 1$ is not well satisfied. For our numerical analysis in the following, we actually use the known loop functions for the top quark and W-boson loop corrections.

In our model, the KK mode mass spectrum of the W-boson is given by

$$m_{n,W}^{(\pm)} = m_n \pm m_W, \tag{24}$$

so that the contribution from KK W-boson loop diagrams is found to be

$$\begin{aligned} C_{\gamma\gamma}^{\rm KKW} &= \frac{e^2}{32\pi^2 v} b_1^W \sum_{n=1}^{\infty}\frac{\partial}{\partial \log v}\left[\log(m_n+m_W)+\log(m_n-m_W)\right] \\ &\simeq \frac{7\alpha_{em}}{8\pi v}\frac{\pi^2}{3}\left(\frac{m_W}{M_{\rm KK}}\right)^2. \end{aligned} \tag{25}$$

Note again that the KK W-boson contribution is destructive to the SM W-boson contribution.

Finally, the **10**-plet or **15**-plet loop contributions can be read from the KK-mode mass spectrum in Eqs. (6) or (8) and the electric charges of each modes:

$$\begin{aligned} C_{\gamma\gamma}^{\rm KK10} &\simeq (Q-1)^2\hat{F}(3m_W)+(Q-1)^2\hat{F}(m_W)+Q^2\hat{F}(2m_W)+(Q+1)^2\hat{F}(m_W), \quad (26)\\ C_{\gamma\gamma}^{\rm KK15} &\simeq (Q-4/3)^2\hat{F}(4m_W)+(Q-4/3)^2\hat{F}(2m_W)+(Q-1/3)^2\hat{F}(3m_W)\\ &\quad +(Q-1/3)^2\hat{F}(m_W)+(Q+2/3)^2\hat{F}(2m_W)+(Q+5/3)^2\hat{F}(m_W) \quad (27)\end{aligned}$$

where Q is a $U(1)'$ charge for the **10** and **15**-plets, and

$$\hat{F}(m_W) \simeq -\frac{\alpha_{em}}{2\pi v}\left(\frac{m_W}{M_{\rm KK}}\right)^2 \frac{\pi^2}{\cosh(\pi c_B)}. \quad (28)$$

Putting all together, we find the ratio of the partial decay width of $h\to\gamma\gamma$ in our model to the SM one as

$$\begin{aligned} R_{\gamma\gamma} &\equiv \left(1+\frac{C_{\gamma\gamma}^{\rm KKtop}+C_{\gamma\gamma}^{\rm KKW}+C_{\gamma\gamma}^{\rm KK10(15)}}{C_{\gamma\gamma}^{\rm SMtop}+C_{\gamma\gamma}^{W}}\right)^2\\ &\simeq \begin{cases} \left(1+\frac{\pi^2}{141}\left(\frac{m_W}{M_{\rm KK}}\right)^2+\left[(3^2+1^2)(Q-1)^2+4Q^2+(Q+1)^2\right]\left(\frac{m_W}{M_{\rm KK}}\right)^2\frac{36\pi^2}{47\cosh(\pi c_B)}\right)^2 \\ \qquad\qquad\qquad\qquad\qquad\qquad\qquad\qquad \text{for } \mathbf{10}-\text{plet.} \\ \left(1+\frac{\pi^2}{141}\left(\frac{m_W}{M_{\rm KK}}\right)^2+\left[(4^2+2^2)\left(Q-\frac{4}{3}\right)^2+(3^2+1^2)\left(Q-\frac{1}{3}\right)^2\right.\right. \\ \qquad\qquad \left.\left.+\,2^2\left(Q+\frac{2}{3}\right)^2+\left(Q+\frac{5}{3}\right)^2\right]\left(\frac{m_W}{M_{\rm KK}}\right)^2\frac{36\pi^2}{47\cosh(\pi c_B)}\right)^2 \text{ for } \mathbf{15}-\text{plet.} \end{cases} \end{aligned} \quad (29)$$

For a fixed Q, the KK mode contributions becomes larger as $M_{\rm KK}$ goes down. As expected, a large $|Q|\gg 1$ significantly alters $R_{\gamma\gamma}$ from 1, for a fixed $M_{\rm KK}$.

Although the $U(1)'$ charge Q is a free parameter of the model, we have phenomenologically favored values for it from the following discussion. As discussed in [24] (see also [25]), the lightest KK mode of the half-periodic bulk fermion, independently of the background metric, is stable in the effective 4-dimensional theory due to the accidental Z_2 discrete symmetry. However, a colored stable particle is cosmologically disfavored.

An easy way to solve this phenomenological problem is to introduce a mixing between the lightest colored KK fermion and a SM quark on the brane, so that the lightest KK fermion can decay to the SM quarks. There are two choices for the $U(1)'$ charge to make the electric charge of the lightest KK mode to be $-1/3$ or $2/3$ for realizing a mixing with either the down-type quarks or up-type quarks. For the **10**-plet case we choose $Q = 2/3$ or $5/3$, while $Q = 1$ or 2 for the **15**-plet case. Fig. 4 shows the results for $R_{\gamma\gamma}$ as a function of $M_{\rm KK}$ for the **10** and **15**-plet cases with the choices, $Q = 2/3$ or $5/3$ and $Q = 1$ or 2, respectively. Here the bulk mass terms are fixed along the lines in Fig. 2 so as to give $m_h = 125$ GeV.

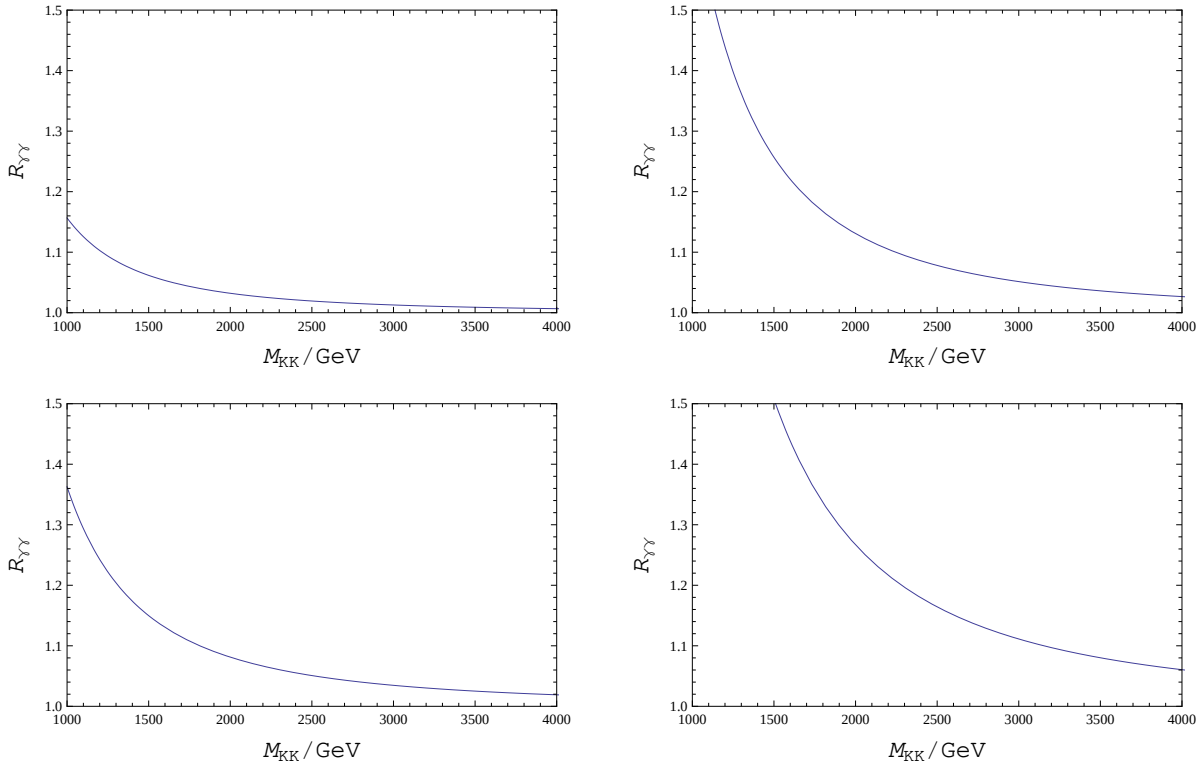


Figure 4: The ratio $R_{\gamma\gamma}$ for the **10**-plet case (upper panels) and the **15**-plet case (lower panels) as a function of $M_{\rm KK}$ with the relations between the bulk mass and $M_{\rm KK}$ depicted in Fig. 2. We have fixed $Q = 2/3$ ($Q = 5/3$) for the upper-left (upper-right) panel in the **10**-plet case (upper panels), while $Q = 1$ ($Q = 2$) for the lower-left (lower-right) panel in the **15**-plet case.

3.3 $gg \to h \to \gamma\gamma$

Let us finally calculate the ratio of the signal strength of the process $gg \to h \to \gamma\gamma$ in our model to the SM one. For the **10**-plet, we have

$$\begin{aligned} \mathrm{R} &\equiv \frac{\sigma(gg \to h \to \gamma\gamma)}{\sigma(gg \to h \to \gamma\gamma)_{\mathrm{SM}}} = R_{gg} \times R_{\gamma\gamma} \\ &\simeq 1 - \frac{374}{141}\pi^2 \left(\frac{m_W}{M_{\mathrm{KK}}}\right)^2 \\ &\quad + \left[-30 + \frac{72}{47}\left\{10(Q-1)^2 + 4Q^2 + (Q+1)^2\right\}\right] \left(\frac{m_W}{M_{\mathrm{KK}}}\right)^2 \frac{\pi^2}{\cosh(\pi c_B)}, \end{aligned} \tag{30}$$

while for the **15**-plet

$$\begin{aligned} \mathrm{R} &\simeq 1 - \frac{374}{141}\pi^2 \left(\frac{m_W}{M_{\mathrm{KK}}}\right)^2 + \left[-50 + \frac{72}{47}\left\{20\left(Q - \frac{4}{3}\right)^2\right.\right. \\ &\quad \left.\left. +10\left(Q - \frac{1}{3}\right)^2 + 4\left(Q + \frac{2}{3}\right)^2 + \left(Q + \frac{5}{3}\right)^2\right\}\right] \left(\frac{m_W}{M_{\mathrm{KK}}}\right)^2 \frac{\pi^2}{\cosh(\pi c_B)}. \end{aligned} \tag{31}$$

For the two cases, we plot the ratio R as a function of the compactification scale M_{KK} in Fig. 5. The upper two panels corresponds to the **10**-plet case, where we have fixed $Q = 2/3$ ($Q = 5/3$) in the upper-left (upper-right) panel. The lower two panels corresponds to the **15**-plet case, where we have fixed $Q = 1$ ($Q = 2$) in the lower-left (lower-right) panel. Comparing Fig. 5 with Fig. 3, we can see that the ratio R is mainly controlled by the Higgs production cross section in Fig. 3, and the signal strength of the diphoton events is smaller than the SM expectation.

4 KK mode fermions at the LHC

Since the mass of the lightest KK mode fermions of the **10** and **15**-plets can be as low as a few TeV, the colored fermions are accessible to the LHC run II with the upgraded collider energy $\sqrt{s} = 13 - 14$ TeV. We have assigned the $U(1)'$ charge so as for the lightest KK mode fermions to have the electric charge of either $-1/3$ or $2/3$ and hence to decay to the SM quarks. When the lightest KK mode fermions couple mainly with the third generation quarks, the LHC phenomenology for them is similar to the one for the

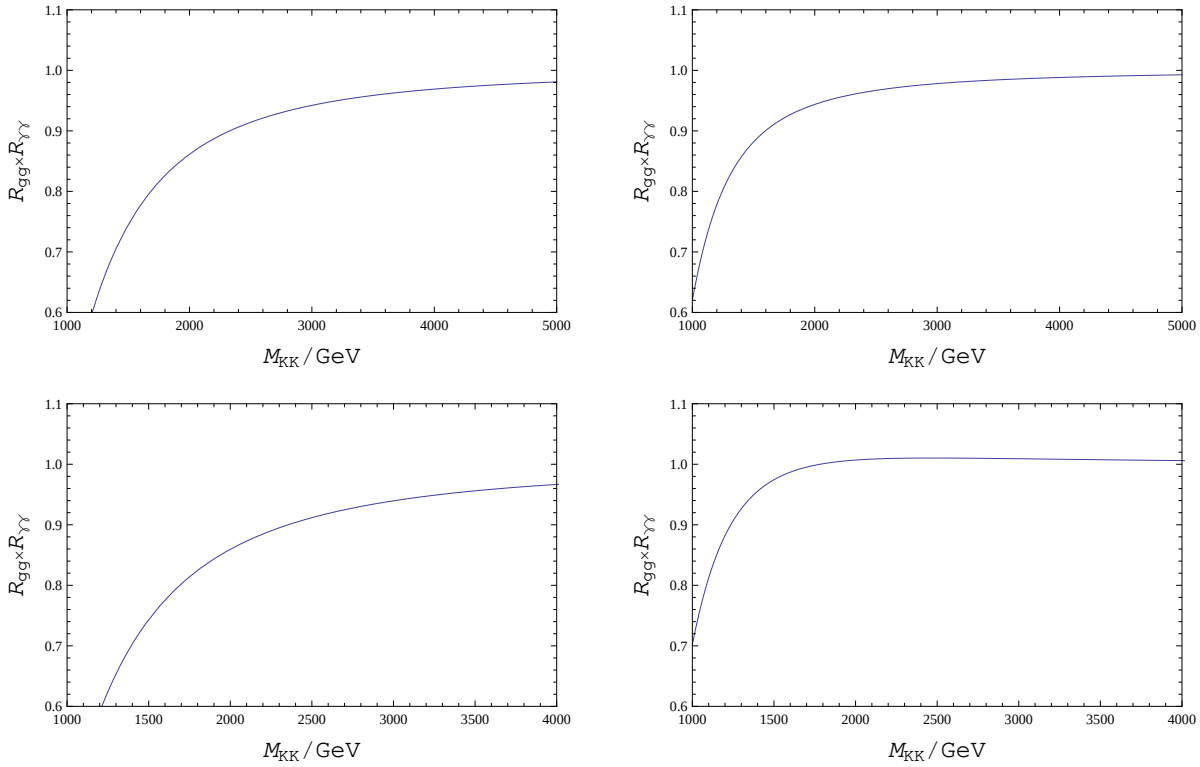


Figure 5: The diphoton signal strength normalized by the SM prediction in the GHU model with the **10**-plet bulk fermions (upper panels) and the **15**-plet bulk fermions (lower panels) as a function of $M_{\rm KK}$. The $U(1)'$ charge of the lightest KK mode fermion in the **10**-plet is fixed to be $Q = 2/3$ ($Q = 5/3$) for the upper-left (upper-right) panel. For the **15**-plet case, we have fixed $Q = 1$ ($Q = 2$) for the lower-left (lower-right) panel.

4th generation quarks. The KK mode fermions, once produced dominantly through the gluon fusion process, decay to the W-boson/Z-boson/Higgs boson and top/bottom quark through the charged/neutral current. See, for example, [26] for the current limit on the heavy quarks at the LHC.

Note that in our model the bulk fermions has been introduced as the **10**-plet or the **15**-plet, and 10 or 15 fermion mass eigenstates appear after the electroweak symmetry breaking, as described in Eqs. (6) and (8). Therefore, if $m_0^{(\pm)}$ is low enough, say, ≤ 3 TeV heavy colored particles with a variety of electromagnetic charges can be produced at the LHC run II. Since the mass eigenstates couples with each other through the weak gauge bosons, a heavy fermion, once produced at the LHC, causes cascade decays to lighter

mass eigenstates and the weak gauge boson, which end up with the lightest KK mode fermion, followed by the decay to the SM quark through the charged/neutral currents. The existence of the variety of fermion mass eigenstates and their cascade decay once produced at the LHC are characteristic feature of our GHU model. Fig. 6 sketches the interactions among the various mass eigenstates for the **10**-plet case. In the figure, we can see a characteristic structure of the interactions among the mass eigenstates and the Z-boson, namely, the Z-boson only couples with two different mass eigenstates. As has been pointed out in [15], there is no KK mode contribution to the effective Higgs-to-$Z\gamma$ in the GHU, because of this characteristic coupling manner.

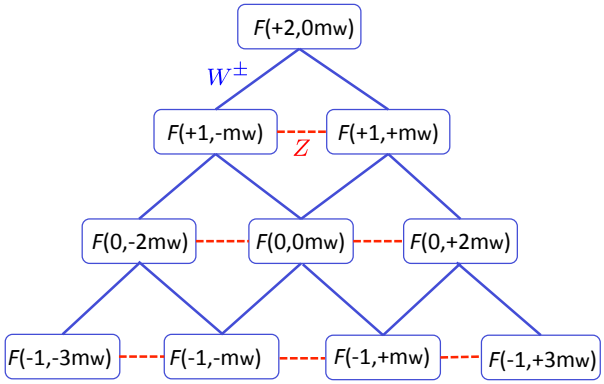


Figure 6: A sketch of the interactions among the mass eigenstates for the **10**-plet case. The diagonal (solid) lines represent the interactions between the connected two mass eigenstates and the W-boson, while the horizontal (dashed) lines represent the interactions between the connected two mass eigenstates and the Z-boson. Here the symbol $F(q, \alpha m_W)$ denotes the mass eigenstate corresponding to the mass eigenvalue in Eq. (6). For example, the mass eigenstate $F(-1, 3m_W)$ has the mass squared eigenvalue of $(m_{\frac{1}{2}} + 3m_W)^2 + M^2$.

5 Conclusions

In this paper, we have performed the Higgs boson mass analysis in a 5-dimensional $SU(3)\times U(1)'$ GHU model. In order to obtain the 125 GeV Higgs mass, we have extended a simple GHU model by introducing colored bulk fermions with a half-periodic boundary condition

and bulk masses. For concreteness, we have considered the fermions in the **6**, **8**, **10** and **15**-plets of $SU(3)$ with a $U(1)'$ charge Q. Employing the gauge-Higgs condition, we have shown in the RGE analysis that the 125 GeV Higgs boson mass can be realized in the presence of the half-periodic bulk fermions by adjusting their bulk masses. Our interest is how the bulk masses can be lowered so that the lightest KK mode fermion might be detectable by the LHC run II. In this regard, the cases with the **6** and **8**-plets are not attractive since the lightest KK mode masses are required to be $\gtrsim 4$ TeV in order to reproduce the 125 GeV Higgs boson mass. On the other hand, the lightest KK mode masses being even less than 1 TeV can achieve $m_h = 125$ GeV in the **10** and **15**-plet cases. Thus, we have focused on these two cases.

The KK mode fermions of the **10** and **15**-plets have contributions to the Higgs-to-digluon and Higgs-to-diphoton couplings. We have evaluated the contributions and found that the Higgs boson production cross section is reduced as the mass of the lightest KK mode fermions becomes lighter. Thus, the LHC results can be used to derive the lower bound on the lightest KK mode mass to be consistent with the LHC data. When $5 - 10$ % reduction of the production cross section is required, we have found the lower bound at a few TeV, reproducing the 125 GeV Higgs boson mass. The colored KK mode fermions with a few TeV masses are accessible to the LHC run II. The $U(1)'$ charges for the lightest KK mode fermions are assigned to be either $-1/3$ or $2/3$, so that they can decay to the SM quarks through the mass mixing introduced on the brane. For the charge assignment, the KK mode fermion contributions to the signal strength of the Higgs-to-diphoton evens are mainly controlled by the Higgs production cross section. LHC phenomenology for the KK mode fermions are similar to the one for the 4th generation heavy quarks, but our model includes more exotic quarks with a variety of masses and electric charges, which originates form the **10** or **15**-plets. Once a heavy KK mode fermion is produced at the LHC, it decays to lighter mass eigenstates. This cascade decay ends up with the lightest KK mode fermion, followed by its decay to the SM quark and the weak boson/Higgs boson. Search for the KK mode fermions at the LHC run II is an interesting topic and we leave it for future work.

Acknowledgments

The work of N.M. is supported in part by the Grant-in-Aid for Scientific Research from the Ministry of Education, Science and Culture, Japan No. 24540283. The work of N.O. is supported in part by the DOE Grant No. DE-FG02-10ER41714.

References

[1] G. Aad *et al.* [ATLAS Collaboration], Phys. Lett. B **716**, 1 (2012).

[2] S. Chatrchyan *et al.* [CMS Collaboration], Phys. Lett. B **716**, 30 (2012).

[3] M. Carena, S. Gori, N. R. Shah and C. E. M. Wagner, JHEP **1203**, 014 (2012); JHEP **1302**, 114 (2013). J. -J. Cao, Z. -X. Heng, J. M. Yang, Y. -M. Zhang and J. -Y. Zhu, JHEP **1203**, 086 (2012); M. Carena, S. Gori, N. R. Shah, C. E. M. Wagner and L. -T. Wang, JHEP **1207**, 175 (2012); H. An, T. Liu and L. -T. Wang, Phys. Rev. D **86**, 075030 (2012); N. Haba, K. Kaneta, Y. Mimura and R. Takahashi, Phys. Lett. B **718**, 1441 (2013). M. A. Ajaib, I. Gogoladze and Q. Shafi, Phys. Rev. D **86**, 095028 (2012); K. Schmidt-Hoberg and F. Staub, JHEP **1210**, 195 (2012); R. Sato, K. Tobioka and N. Yokozaki, Phys. Lett. B **716**, 441 (2012); T. Kitahara, JHEP **1211**, 021 (2012); M. Berg, I. Buchberger, D. M. Ghilencea and C. Petersson, Phys. Rev. D **88**, 025017 (2013); J. Cao, L. Wu, P. Wu and J. M. Yang, JHEP **1309**, 043 (2013); B. Batell, S. Jung and C. E. M. Wagner, arXiv:1309.2297 [hep-ph].

[4] J. S. Gainer, W. -Y. Keung, I. Low and P. Schwaller, Phys. Rev. D **86**, 033010 (2012); B. Batell, S. Gori and L. -T. Wang, JHEP **1206**, 172 (2012); S. Kanemura and K. Yagyu, Phys. Rev. D **85**, 115009 (2012); L. Wang and X. -F. Han, JHEP **1205**, 088 (2012); A. G. Akeroyd and S. Moretti, Phys. Rev. D **86**, 035015 (2012); W. -F. Chang, J. N. Ng and J. M. S. Wu, Phys. Rev. D **86**, 033003 (2012); M. Carena, I. Low and C. E. M. Wagner, JHEP **1208**, 060 (2012); A. Alves, A. G. Dias, E. Ramirez Barreto, C. A. de S.Pires, F. S. Queiroz and P. S. Rodrigues da Silva, Eur. Phys. J. C **73**, 2288 (2013); T. Abe, N. Chen and H. -J. He, JHEP

1301, 082 (2013); A. Joglekar, P. Schwaller and C. E. M. Wagner, JHEP **1212**, 064 (2012); N. Arkani-Hamed, K. Blum, R. T. D'Agnolo and J. Fan, JHEP **1301**, 149 (2013). L. G. Almeida, E. Bertuzzo, P. A. N. Machado and R. Z. Funchal, JHEP **1211**, 085 (2012); M. Hashimoto and V. A. Miransky, Phys. Rev. D **86**, 095018 (2012); M. Reece, New J. Phys. **15**, 043003 (2013). H. Davoudiasl, H. -S. Lee and W. J. Marciano, Phys. Rev. D **86**, 095009 (2012); M. B. Voloshin, Phys. Rev. D **86**, 093016 (2012); A. Kobakhidze, arXiv:1208.5180 [hep-ph]; A. Urbano, Phys. Rev. D **87**, 053003 (2013). L. Wang and X. -F. Han, Phys. Rev. D **87**, 015015 (2013); E. J. Chun, H. M. Lee and P. Sharma, JHEP **1211**, 106 (2012); H. M. Lee, M. Park and W. -I. Park, JHEP **1212**, 037 (2012); B. Batell, S. Gori and L. -T. Wang, JHEP **1301**, 139 (2013). M. Chala, JHEP **1301**, 122 (2013). arXiv:1210.6208 [hep-ph]; B. Batell, S. Jung and H. M. Lee, JHEP **1301**, 135 (2013). C. -W. Chiang and K. Yagyu, JHEP **1301**, 026 (2013). H. Davoudiasl, I. Lewis and E. Ponton, Phys. Rev. D **87**, 093001 (2013); M. Aoki, S. Kanemura, M. Kikuchi and K. Yagyu, Phys. Rev. D **87**, 015012 (2013). F. Arbabifar, S. Bahrami and M. Frank, Phys. Rev. D **87**, 015020 (2013). S. Funatsu, H. Hatanaka, Y. Hosotani, Y. Orikasa and T. Shimotani, Phys. Lett. B **722**, 94 (2013). P. S. B. Dev, D. K. Ghosh, N. Okada and I. Saha, JHEP **1303**, 150 (2013). A. Carmona and F. Goertz, JHEP **1304**, 163 (2013); N. Okada and T. Yamada, arXiv:1304.2962 [hep-ph]; C. -X. Yue, Q. -Y. Shi and T. Hua, arXiv:1307.5572 [hep-ph]. W. Altmannshofer, M. Bauer and M. Carena, arXiv:1308.1987 [hep-ph]; S. Bahrami and M. Frank, arXiv:1308.2847 [hep-ph]; D. Bunk, J. Hubisz and B. Jain, arXiv:1309.7988 [hep-ph].

[5] The ATLAS Collaboration, ATLAS-CONF-2013-012.

[6] The CMS Collaboration, CMS-PAS-HIG-13-001.

[7] N. S. Manton, Nucl. Phys. B **158**, 141 (1979); D. B. Fairlie, Phys. Lett. B **82**, 97 (1979), J. Phys. G **5**, L55 (1979); Y. Hosotani, Phys. Lett. B **126**, 309 (1983), Phys. Lett. B **129**, 193 (1983), Annals Phys. **190**, 233 (1989).

[8] I. Antoniadis, K. Benakli and M. Quiros, New J. Phys. **3**, 20 (2001); G. von Gersdorff, N. Irges and M. Quiros, Nucl. Phys. B **635**, 127 (2002); R. Contino, Y. Nomura and A. Pomarol, Nucl. Phys. B **671**, 148 (2003); C. S. Lim, N. Maru and K. Hasegawa, J. Phys. Soc. Jap. **77**, 074101 (2008).

[9] N. Maru and T. Yamashita, Nucl. Phys. B **754**, 127 (2006); Y. Hosotani, N. Maru, K. Takenaga and T. Yamashita, Prog. Theor. Phys. **118**, 1053 (2007).

[10] N. Maru and N. Okada, Phys. Rev. D **77**, 055010 (2008).

[11] N. Maru, Mod. Phys. Lett. A **23**, 2737 (2008).

[12] N. Maru and N. Okada, Phys. Rev. D **87**, 095019 (2013).

[13] Y. Adachi, C. S. Lim and N. Maru, Phys. Rev. D **76**, 075009 (2007); Phys. Rev. D **79**, 075018 (2009).

[14] Y. Adachi, C. S. Lim and N. Maru, Phys. Rev. D **80**, 055025 (2009).

[15] N. Maru and N. Okada, Phys. Rev. D **88**, 037701 (2013).

[16] C. A. Scrucca, M. Serone and L. Silvestrini, Nucl. Phys. B **669**, 128 (2003).

[17] G. Cacciapaglia, C. Csaki and S. C. Park, JHEP **0603**, 099 (2006).

[18] N. Haba, S. Matsumoto, N. Okada and T. Yamashita, JHEP **0602**, 073 (2006); Prog. Theor. Phys. **120**, 77 (2008).

[19] Y. Adachi, N. Kurahashi, C. S. Lim and N. Maru, JHEP **1011**, 150 (2010); JHEP **1201**, 047 (2012); Y. Adachi, N. Kurahashi, N. Maru and K. Tanabe, Phys. Rev. D **85**, 096001 (2012); arXiv:1201.2290 [hep-ph]; C. S. Lim, N. Maru and K. Nishiwaki, Phys. Rev. D **81**, 076006 (2010).

[20] I. Gogoladze, N. Okada and Q. Shafi, Phys. Lett. B **655**, 257 (2007); Phys. Lett. B **659**, 316 (2008); B. He, N. Okada and Q. Shafi, Phys. Lett. B **716**, 197 (2012).

[21] For a recent work, see, for example, G. Degrassi, S. Di Vita, J. Elias-Miro, J. R. Espinosa, G. F. Giudice, G. Isidori and A. Strumia, JHEP **1208**, 098 (2012).

[22] J. R. Ellis, M. K. Gaillard and D. V. Nanopoulos, Nucl. Phys. B **106**, 292 (1976).

[23] F. J. Petriello, JHEP **0205**, 003 (2002); S. K. Rai, Int. J. Mod. Phys. A **23**, 823 (2008).

[24] N. Haba, S. Matsumoto, N. Okada and T. Yamashita, JHEP **1003**, 064 (2010).

[25] M. Regis, M. Serone and P. Ullio, JHEP **0703**, 084 (2007); G. Panico, E. Ponton, J. Santiago and M. Serone, Phys. Rev. D **77**, 115012 (2008); M. Carena, A. D. Medina, N. R. Shah and C. E. M. Wagner, Phys. Rev. D **79**, 096010 (2009) ; Y. Hosotani, P. Ko and M. Tanaka, Phys. Lett. B **680**, 179 (2009).

[26] See, for example, A. Ivanov [CMS Collaboration], arXiv:1308.3084 [hep-ex].